Organic LETTERS

Letter

pubs.acs.org/OrgLett

Triindole-Bridge-Triindole Dimers as Models for Two Dimensional Microporous Polymers

Constanza Ruiz,[†] Juan T. López Navarrete,[‡] M. Carmen Ruiz Delgado,*[,‡] and Berta Gómez-Lor*[,†]

[†]Instituto de Ciencia de Materiales de Madrid, CSIC, Cantoblanco 28049, Madrid, Spain

[‡]Department of Physical Chemistry, University of Málaga, 29071 Málaga, Spain

Supporting Information

ABSTRACT: New dimers with two triindole subunits bound together through different linkers (*p*-phenylene or diacetylene groups) have been synthesized and studied as model systems to determine the differences in the electron transfer ability of the two bridging units. Our results show that whereas a *p*-phenylene bridge nearly isolates the two subunits of the dimers a diacetylene bridge allows a high level of electronic connection between them.

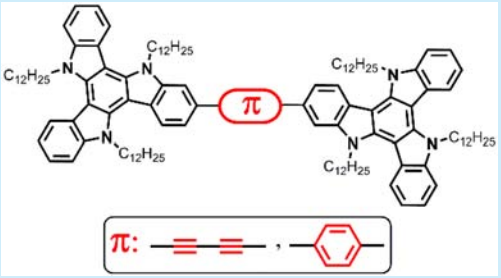

During the past decade, heptacyclic 10,15-dihydro-5*H*-diindolo[3,2-a:3′,2′-c]carbazole (triindole) has been extensively studied as a new π-conjugated platform in the construction of dendrimers and self-assembling materials for optoelectronics due to its strong light emission[1] and efficient charge transport properties.[2,3] Especially remarkable is the record hole mobility values determined on triindole-based semiconducting liquid crystals as a result of the favorable synergy between the intrinsic properties of the platform and its supramolecular arrangement.[3] This molecule has also recently been explored as the functional component in a microporous chemosensing polymer.[4]

Covalent microporous polymers constituted by π-conjugated building units have emerged as a new kind of organic material for electronic applications.[5] In this type of material, the covalent linkage of functional π-conjugated components gives rise to two-dimensional (2D) layers, among which π -π stacking interactions can induce additional order while their intrinsic porosity offers significant opportunities to incorporate guests/chemicals to tune their functionalities. Potential applications have been demonstrated, such as light harvesting,[6] luminescence,[7] sensing,[4] photochemical water splitting,[8] and charge transport.[9] For optoelectronic applications, it is highly desirable that the π-conjugation spans the 2D sheets; however, in covalent microporous polymers, electronic conjugation is often limited to the constituent building π-functional units. The degree of lateral conjugation and electronic coupling is highly dependent upon the nature of the bridge that connects the individual interacting components and has a profound effect on the behavior of excitons and charge carriers. In spite of the impressive progress that this field has experienced during the past few years, the insoluble character of covalent microporous polymers limits detailed postsynthetic studies to investigate how the structure will affect the desired properties and thus the design of optimal polymeric materials on a molecular basis. Note that examples of soluble conjugated microporous polymers reported to date are quite scarce.[10] Discrete low-molecular weight oligomers with well-defined chemical structures may represent invaluable models to establish clear structure−property relationships, therefore avoiding insolubility, irreproducibility issues, and variations from batch-to-batch, which are common drawbacks in polymeric materials.

To facilitate the design of new triindole-based polymeric materials on a molecular basis and establish clear guidelines to fine-tune parameters, such as energy gap, light absorption, and light emitting properties, we have synthesized two new dimers in which the two triindole molecules are linked by *p*-phenylene or diacetylene bridges. The present work aims to investigate the influence of the π-bridge in the electronic communication between the two triindole groups. To this end, we performed a detailed study of the electronic and photophysical properties of the new dimers and their monomeric analogues using absorption, emission, and Raman spectroscopies, cyclic voltammetry, and DFT calculations.

The synthesis of the two dimeric molecules has been performed starting from 2-monobromo-*N*-dodecyltriindole. This molecule has been obtained by bromination of *N*-dodecyltriindole **1** with 1 equiv of NBS under high-dilution conditions. Under these conditions, compound **2** is obtained along with some dibrominated derivatives. It should be noted that this molecule has been previously wrongly assigned as 3-monobromotriindole.[11] The unambiguous characterization of this molecule has been performed by MS, ^{1}H and ^{13}CNMR, as well as HMBC and HMQC 2D experiments (see Supporting Information).[12] Compound **6**, with two triindole units separated by a phenylene linker, was obtained by a

Received: March 27, 2015
Published: April 20, 2015

DOI: 10.1021/acs.orglett.5b00900
Org. Lett. 2015, 17, 2258−2261

palladium-catalyzed Suzuki cross-coupling reaction between 2 equiv of 2-bromotriindole **2** and 1 equiv of benzene 1,4-diboronic acid. Separately, compound **7** was obtained by Glaser homocoupling of 1-ethynyltrindol **5** (obtained by Sonogashira coupling of the monobrominated precursor with TMS acetylene to render **4**, followed by deprotection with NaOH).

Scheme 1. Synthesis of Dimeric Molecules 6 and 7 and Their Monomer Analogues 3 and 5, Respectively

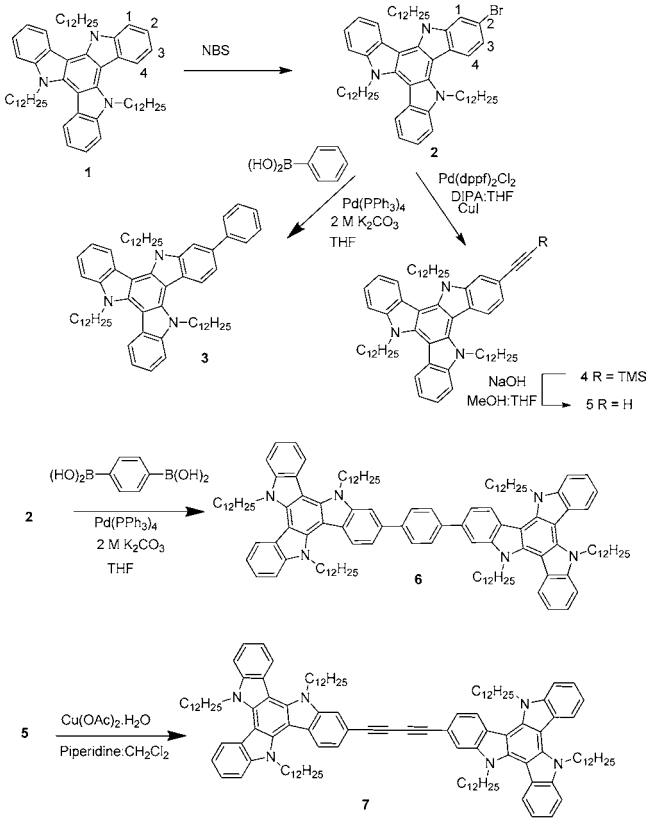

As shown in Figure 1 and Table 1, the electronic absorption maxima and the absorption edge of **3** and **5** monomers are slightly red-shifted when compared to the unsubstituted triindole **1** with both ethynyl and phenyl substituents exerting a very similar effect. This HOMO−LUMO gap decrease is associated with stabilization of the LUMO upon insertion of the ethynyl or phenyl groups, while the HOMO energies are slightly affected; note that the LUMOs of **3** and **5** are more localized at the external ethynyl or phenyl groups, whereas their HOMOs are delocalized over the entire molecular π-frameworks (see Figure S1, Supporting Information). However, when going from the monomers to the dimers, the overall shapes of the electronic spectra change with the appearance of a new band at a longer wavelength and a significant red-shift of the absorption edge with this effect being more significant in the diacetylene-bridged triindole dimer **7** (see Figure 1). Time-dependent DFT vertical excitation energies are in agreement with the experimental data and predict that this band is associated with a HOMO → LUMO one-electron excitation (see Table 1 and Figure S2, Supporting Information). As evidenced by the frontier molecular orbitals of dimers **6** and **7** shown in Figure 2, the lowest-energy electronic transition has a certain charge-transfer character (i.e., the HOMOs are delocalized over the entire molecular π-frameworks whereas the LUMOs are more localized at the central spacer) thus resulting in a HOMO−LUMO decrease. This effect is more pronounced in **7** due to the electron-accepting character and cylindrical symmetry of the diacetylenic spacer, which allows

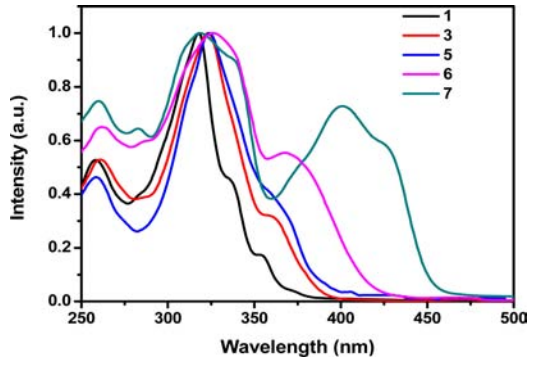

Figure 1. Experimental UV−vis spectra of unsubstituted **1**, monomers **3** and **5**, and dimers **6** and **7** in CH_2Cl_2, $c = 5 \times 10^{-6}$ M.

Table 1. Optical and Fluorescence Properties

	HOMO[a] (eV)	LUMO[a] (eV)	$\lambda_{(abs)}$[b] (nm)	$\lambda_{(abs,calc)}$[c] (nm)	$\lambda_{(em)}$ (nm)	Φ_{PL}[d] (%)
1	−5.05	−1.78	318 (4.19)	312 (f = 0.46)	397	0.23
3	−5.05	−1.93	320 (5.10)	353 (f = 0.30)	421	0.50
5	−5.13	−1.97	322 (4.90)	352 (f = 0.21)	427	0.47
6	−5.06	−2.07	326 (5.01)	390 (f = 1.66)	447	0.48
7	−5.08	−2.39	318 (5.23)	444 (f = 2.38)	468	0.42

[a]The HOMO energy values for **1** to **7** were estimated from the first oxidation potential with respect to the ferrocene/ferrocenium redox couple. The LUMO energy values were estimated by subtracting the energy of the optical band gap obtained by UV−vis from the HOMO values. [b]Absorbance (log ε) values are given in parentheses. [c]Absorption maxima calculated at the B3LYP/6-31G** level within the TD-DFT approach. Oscillator strengths (f) are given in parentheses. [d]Fluorescence quantum yields are relative to quinine hemisulfate.

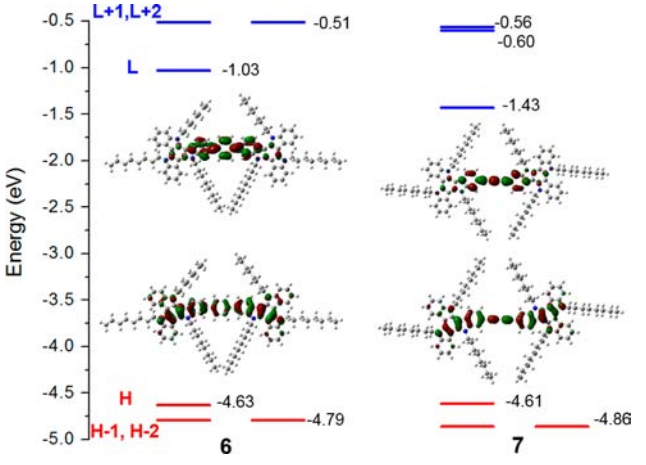

Figure 2. DFT-calculated molecular orbital energies (B3LYP/6-31G** level) for dimers **6** and **7**. The topologies of the frontier molecular orbitals are also shown.

DOI: 10.1021/acs.orglett.5b00900
Org. Lett. 2015, 17, 2258−2261

for better extension of π-conjugation.[13] In fact, the rotation around the triindole moieties and the central spacer has been explored by DFT calculations (see Figure S3, Supporting Information), and a rather flat torsional potential is found for the diacetylenic-bridged dimer **7** with a very small energy difference (0.32 kcal/mol) between the perpendicular conformation and the most stable *trans* coplanar conformer. The coexistence of these two conformers at room temperature has also been confirmed by temperature-dependent absorption spectra measurements (see Supporting Information). However, the most stable conformation of dimer **6** corresponds to a moderately distorted configuration, where the central phenyl ring is rotated by 36° with respect to the triindole moieties, which is thus less favorable toward π-electron delocalization than that of the diacetylenic spacer.

Next, the effective π-conjugation of the triindole dimers are investigated by Raman spectroscopy. As seen in Figure 3, the

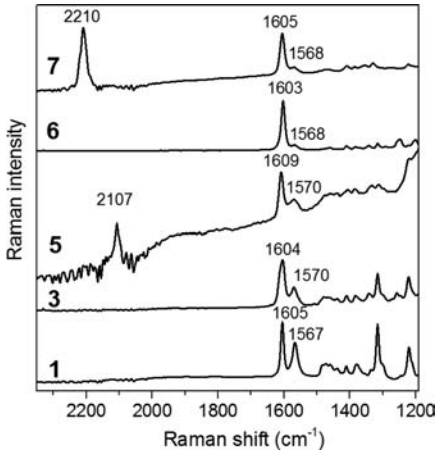

Figure 3. Experimental Raman spectra of unsubstituted **1**, monomers **3** and **5**, and dimers **6** and **7**.

strongest Raman band of triindole molecules is measured at ~1605 cm^{-1} and arises from a CC stretching mode (i.e., mode 8a of benzene[14]) involving the external benzene rings, whereas the Raman band at ~1567 cm^{-1} is due to the same CC stretching mode but located in the innermost benzene ring. Compared to unsubstituted triindole **1**, this doublet band increases in intensity in the monomers and dimers with respect to the rest of the bands recorded below 1500 cm^{-1}. A frequency downshift of this doublet and an increase in the I_{1605}/I_{1567} intensity ratio is also found in the following order: unsubstituted **1** < monofunctionalized monomers **3** and **5** < dimers **6** and **7**. This indicates more efficient π-conjugation in the dimers, which is in consonance with their larger geometrical relaxation when compared to the monomers (see Figure S4, Supporting Information). In diacetylenic-bridged dimer **7**, the most intense Raman band measured at 2210 cm^{-1} is described as fully in-phase C≡C stretching vibrations and evidences the strong participation of the diacetylenic bridge in the overall π-conjugation. The increase of the intensity of this band with respect to that associated with the central benzene rings (1605 cm^{-1}) in dimer **7** compared to monomer **5** is indicative that π-conjugation takes place more efficiently in the central part of the molecules and decreases toward the ends. The good agreement found between the theoretical and experimental Raman spectra gives support to the reliability of the structural information derived from this discussion (see Figure S5, Supporting Information).

Cyclic voltammetry analysis of these electron-rich triindole platforms shows that all compounds exhibit a first oxidation reversible process, which is associated with the easy generation of a cation radical as well as the formation of higher cationic charged species (see Figure 4 for **6** and **7** dimers and the

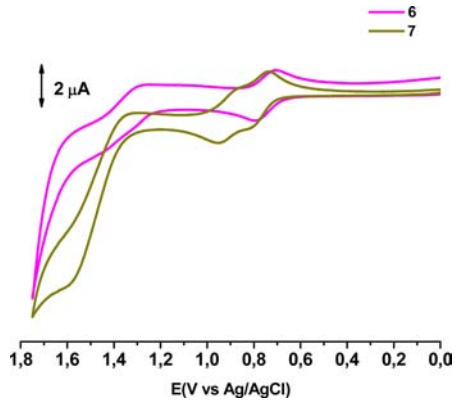

Figure 4. CV of dimers **6** and **7** at $c = 1 \times 10^{-3}$ M, recorded at a scan rate of 100 mV s^{-1} in CH_2Cl_2/0.1 M $TBAPF_6$ measured versus Ag/AgCl (3 M NaCl).

Supporting Information for the rest of the compounds). For the monomeric species, the first oxidation potential is found to slightly shift anodically on going from **3** to **5** as a consequence of the electron-withdrawing effect of the ethynyl group; this is in consonance with the small HOMO stabilization calculated for **5** (Table 1 displays the estimated HOMO levels from the first oxidation waves). For the dimers, the values of the first oxidation process are very similar and are in agreement with the low influence that the two different spacers have on the HOMO levels. However, whereas the cyclic voltammogram of dimer **6** is identical to that of its phenyltriindole monomer analogue **3**, indicating that the two triindole units are electronically isolated, the first oxidation wave of dimer **7** is split into two overlapping waves (Figure 4). This is evidence that, in the diacetylene-bridged system, the two triindole moieties are electronically coupled, allowing for their subsequent oxidation. This is consistent with the DFT calculations that show a larger charge delocalization in radical cation **7** than in **6**, and therefore better electronic conjugation across the diacetylenic group than over the phenyl spacer (see Figure S6, Supporting Information).

The easy one-electron reversible oxidation of the triindole dimers together with their moderate predicted values of hole intramolecular reorganization energy (λ_h) would render them as potential hole-transport material candidates, as previously found in unsubstituted triindoles.[15] Note that λ_h values of 149 and 163 meV are obtained for dimers **6** and **7**, respectively, which are on the same order as those calculated for many other organic systems considered to be good hole-transport materials (i.e., 306 meV was obtained for phenyl-susbtituted dithienoacene for which hole field-effect mobilities as high as 0.31 cm^2 V^{-1} s^{-1} were reported[16]).

An examination of the fluorescence properties (see Table 1) shows two clear effects: (i) a red-shift of the emission maxima is found when going from unsubstituted **1** to monofunctionalized monomers **3** and **5** and dimers **6** and **7** with this being more pronounced in the acetylenic-substituted systems compared to

DOI: 10.1021/acs.orglett.5b00900
Org. Lett. 2015, 17, 2258−2261

the phenyl-substituted analogues, and (ii) an increase in the fluorescence quantum yield is found upon insertion of the linkers with the four derivatives (**3**, **5**, **6**, and **7**) showing similar values.

In summary, we have presented the first systematic investigation focusing on the effects that π-spacers in triindole dimers exert on their fundamental properties, such as electronic, redox, and photophysical properties. Our study demonstrates that the optoelectronic properties of the triindole dimers are strongly influenced by the nature of the π-linkers; the diacetylenic bridge allows for better electronic delocalization. We hope that this study can not only advance useful structure−property relationships of conjugated triindole dimers but also guide the design of new polymeric microporous materials based on this interesting platform.

■ ASSOCIATED CONTENT

Supporting Information

Additional experimental (characterization of monomers **3** and **5** and dimers **6** and **7**, temperature variable absorption spectra of dimer **7**, emission spectra of **1** to **7** systems, cyclic voltammograms of **1**, **3**, and **5**) and theoretical data (molecular orbital energies and topologies of monomers **1**, **3**, and **5**; simulated absorption spectra of neutral species; DFT rotational barriers of dimers **6** and **7**; theoretical Raman spectra of monomers **1**, **3**, and **5** and dimers **6** and **7**; and calculated bond length modifications in the neutral species and upon oxidation). This material is available free of charge via the Internet at http://pubs.acs.org.

■ AUTHOR INFORMATION

Corresponding Authors

*E-mail: carmenrd@uma.es.

* E-mail: bgl@icmm.csic.es.

Notes

The authors declare no competing financial interest.

■ ACKNOWLEDGMENTS

This work was financially supported by the MINECO of Spain (CTQ2012-33733 and CTQ2013-40562-R) and the Comunidad de Madrid S2013/MIT-2740 and Junta de Andalucía (P09-FQM-4708). M.C.R.D. thanks the MICINN for a "Ramón y Cajal" Research contract.

■ REFERENCES

(1) (a) Lai, W. Y.; He, Q. Y.; Zhu, R.; Chen, Q. Q.; Huang, W. *Adv. Funct. Mater.* **2008**, *18*, 265−276. (b) Levermore, P. A.; Xia, R.; Lai, W.; Wang, X. H.; Huang, W.; Bradley, D. D. C. *J. Phys. D: Appl. Phys.* **2007**, *40*, 1896.

(2) (a) García-Frutos, E. M.; Gutierrez-Puebla, E.; Monge, M. A.; Ramírez, R.; Andrés, P. d.; Andrés, A. d.; Gómez-Lor, B. *Org. Electron.* **2009**, *10*, 643. (b) Reig, M.; Puigdollers, J.; Velasco, D. *J. Mater. Chem. C* **2015**, *3*, 506.

(3) (a) Ye, Q.; Chang, J.; Shao, J.; Chi, C. *J. Mater. Chem.* **2012**, *22*, 13180. (b) Benito-Hernández, A.; Pandey, U. K.; Cavero, E.; Termine, R.; García-Frutos, E. M.; Serrano, J. L.; Golemme, A.; Gómez-Lor, B. *Chem. Mater.* **2013**, *25*, 117. (c) García-Frutos, E. M.; Pandey, U. K.; Termine, R.; Omenat, A.; Barberá, J.; Serrano, J. L.; Golemme, A.; Gómez-Lor, B. *Angew. Chem., Int. Ed.* **2011**, *50*, 7399.

(4) Liu, X.; Xu, Y.; Jiang, D. *J. Am. Chem. Soc.* **2012**, *134*, 8738.

(5) (a) Xu, Y.; Jin, S.; Xu, H.; Nagai, A.; Jiang, D. *Chem. Soc. Rev.* **2013**, *42*, 8012−8031. (b) Thomas, H. *Angew. Chem., Int. Ed.* **2010**, *49*, 8328−8344.

(6) Chen, L.; Honsho, Y.; Seki, S.; Jiang, D. *J. Am. Chem. Soc.* **2010**, *132*, 6742−6748.

(7) (a) Jiang, J. X.; Trewin, A.; Adams, D. J.; Cooper, A. I. *Chem. Sci.* **2011**, *2*, 1777−1781. (b) Xu, Y.; Chen, L.; Guo, Z.; Nagai, A.; Jiang, D. *J. Am. Chem. Soc.* **2011**, *133*, 17622−17625.

(8) Sprick, R. S.; Jiang, J.-X.; Bonillo, B.; Ren, S.; Ratvijitvech, T.; Guiglion, P.; Zwijnenburg, M. A.; Adams, D. J.; Cooper, A. I. *J. Am. Chem. Soc.* **2015**, *137*, 3265.

(9) Ding, H.; Li, Y.; Hu, H.; Sun, Y.; Wang, J.; Wang, C.; Wang, C.; Zhang, G.; Wang, B.; Xu, W.; Zhang, D. *Chem.—Eur. J.* **2014**, *20*, 14614−14618. (c) Bildirir, H.; Paraknowitsch, J. P.; Thomas, A. *Chem.—Eur. J.* **2014**, *20*, 9543−9548.

(10) Cheng, G.; Hasell, T.; Trewin, A.; Adams, D. J.; Cooper, A. I. *Angew. Chem., Int. Ed.* **2012**, *51*, 12727.

(11) Bura, T.; Leclerc, N.; Fall, S.; Lévêque, P.; Heiser, T.; Ziessel, R. *Org. Lett.* **2011**, *13*, 6030.

(12) The regioselectivity of the reaction can be understood considering the radical character of the aromatic bromination exerted by NBS. The 2-position bears significantly higher electron density than the 3-position, as has been previously determined by Mulliken population analysis of the electron spin distribution of the triindole radical cation. See reference 2a.

(13) Ruiz Delgado, M. C.; Casado, J.; Hernández, V.; López Navarrete, J. T.; Fuhrmann, G.; Bäuerle, P. *J. Phys. Chem. B* **2004**, *108*, 3158−3167.

(14) Wilson, E. B.; Decius, J. C.; Cross, P. C. *Molecular Vibrations. The Theory of Infrared and Raman Vibrational Spectra*; McGraw-Hill: New York, Toronto, London, 1955.

(15) Ruiz, C.; García-Frutos, E. M.; da Silva Filho, D. A.; López Navarrete, J. T.; Ruiz Delgado, M. C.; Gómez-Lor, B. *J. Phys. Chem. C* **2014**, *118*, 5470−5477.

(16) Sun, Y. M.; Ma, Y. Q.; Liu, Y. Q.; Lin, Y. Y.; Wang, Z. Y.; Wang, Y.; Di, C. A.; Xiao, K.; Chen, X. M.; Qiu, W. F.; Zhang, B.; Yu, G.; Hu, W. P.; Zhu, D. B. *Adv. Funct. Mater.* **2006**, *16*, 426−432.

DOI: 10.1021/acs.orglett.5b00900
Org. Lett. 2015, 17, 2258−2261